

Intrinsic, Narrow N V Absorption Reveals a Clumpy Outflow in $z < 0.4$ Radio-Loud Quasars

Chris Culliton^{1*}, Bryan DeMarcy¹, Viktoriah Serra², Rajib Ganguly², Jessie Runnoe³, Jane Charlton¹, Michael Eracleous¹, Toru Misawa⁴, Anand Narayanan⁵

¹The Pennsylvania State University, 525 Davey Lab, University Park, PA 16802, USA

²University of Michigan-Flint, Murchie Science Building, 303 Kearsley Street, Flint, MI, 48502, USA

³University of Michigan-Ann Arbor, Ann Arbor, MI, United States

⁴Shinshu University, 3-1-1 Asahi, Matsumoto, Nagano, 390-8621, Japan

⁵Indian Institute of Space Science & Technology, Thiruvananthapuram, Kerala, India

Accepted. Received; in original form

ABSTRACT

Quasar outflows are often invoked in models for galaxy evolution to inject energy and momentum into the gas in the host galaxy and influence its star formation history. Thus, the study of quasar outflows is essential for understanding galaxy evolution. N V absorption systems within the associated region ($|\Delta v| \leq 5000 \text{ km s}^{-1}$) of the quasar are thought to be intrinsic since many show evidence for partial covering of the quasar. A recent archival study of quasar spectra taken with COS/G130M or G160M found 48/158 radio-quiet quasars show intrinsic N V absorption, while none of the 16 radio-loud quasars have N V absorption detected (Culliton et al. 2018). Further investigation of these radio-loud quasars showed a clear bias towards compact morphologies as revealed by FIRST 1.4 GHz imaging and comparatively flat radio spectra. This suggests we are viewing more face-on orientations which prevent us from seeing absorption outflows. The cause for such bias within the HST archive is still unknown; however, it could explain the lack of radio-loud intrinsic N V absorption seen by Culliton et al. (2018). Alternatively, the quasar wind structure may be fundamentally different between radio-loud and radio-quiet objects. We used COS/G130M or G160M to obtain rest-frame UV spectra (1195 Å–1250 Å) of 13 low-redshift SDSS radio-loud quasars which show lobe-dominated FIRST morphologies to distinguish between these possibilities. Intrinsic N V absorption was detected in 6 of our 13 quasars. This suggests the lack of detections in the archival study was a result of an orientation effect/sampling bias rather than to differences in wind structure between radio-loud and radio-quiet quasars. We find significant overlap in radio core fractions between quasars with and without N V detection. Quasars in our sample with N V detection span a range of core-to-lobe ratios from < 0.01 up to 8.5 while those without detected N V range from 0.04 up to 14, corresponding to a range of calculated inclination angles with respect to the polar axis from 20° to > 69° while those without detected N V range from 15° up to 61°. A laminar outflow with a small opening angle would be difficult to explain given this overlap in radio core fractions. However, only 2 of the 15 systems found had inclination angles $i < 45^\circ$. The remaining 13 N V absorption systems were found within the spectra of quasars at high inclination angles ($i \geq 50^\circ$). Additionally, each of the quasars with high inclination angles ($i \geq 50^\circ$) that had N V absorption within its spectra were found to have multiple systems, indicating that such systems in high inclination angle quasars tend to cluster. This implies that the probability of finding an intrinsic N V system within a radio-loud quasar increases as the inclination angle increases. Our observations suggest that a clumpy, sporadic outflow is the most likely explanation.

Key words: accretion, accretion discs – galaxies: active – quasars: absorption lines – quasars: general

1 INTRODUCTION

* E-mail: csc189@psu.edu

The study of quasar outflows is essential for our understanding of quasar structure and galaxy evolution. Quasar

outflows can take the form of collimated jets and/or accretion disk winds. These outflows have many affects on the quasar environment, including enriching the intergalactic medium (IGM), and transferring momentum to the interstellar medium (ISM), which can cause the host galaxy's gas and dust to be expelled. This quenches star formation throughout the host galaxy, and causes the galaxy to redshift faster than it would otherwise (Di Matteo et al. 2005; Suresh et al. 2015; Hopkins et al. 2016).

In order to study quasar winds, we must examine the absorption systems from the material that makes up these winds. The absorption lines observed in the spectra of QSOs can arise from a wide variety of objects including Milky Way absorption, intervening galaxies, or the intergalactic medium. We must therefore determine which absorption systems are produced by gas that is intrinsic to the QSO. Broad absorption lines (BALs) with high velocity dispersions ($\Delta v > 2,000 \text{ km s}^{-1}$) and mini-BALs ($500 \text{ km s}^{-1} < \Delta v < 2,000 \text{ km s}^{-1}$) are generally considered to be intrinsic due to the conditions needed for such large velocities. Narrow absorption lines (NALs) with $\Delta v < 500 \text{ km s}^{-1}$ are much harder to classify as intrinsic. Time variability and partial coverage are perhaps the most widely applicable ways to distinguish between an intrinsic and intervening absorber (Barlow et al. 1997). Another indicator that a NAL is intrinsic is the presence of the N V doublet $\lambda\lambda 1239, 1243$. The N V doublet line has a relatively high occurrence rate in intrinsic systems compared to other ions, such as C IV or Si IV. N V absorption lines are also rarely seen outside of the associated region ($|\Delta v| < 5,000 \text{ km s}^{-1}$, even when the Ly α forest is not present, which is indicative of a physical association with the quasar. N V NALs tend to have velocity structures indicative of an intrinsic system, and also have high ionization levels. All of these factors lead to N V absorption systems likely being intrinsic to the host quasar.

The rate of occurrence of these intrinsic systems has been shown to depend on the properties of the quasar. Radio-quiet quasars that are soft X-ray weak have been found to be more likely to contain intrinsic absorption systems than other types of quasars (Ganguly et al. 2001). Statistical excesses of C IV doublet lines within the associated region of radio-loud, steep-spectrum quasars have been observed, despite radio-loud, flat-spectrum quasars showing no such excess (Weymann et al. 1979; Young et al. 1982; Foltz et al. 1986; Anderson et al. 1987; Sargent et al. 1988; Ganguly et al. 2001).

Culliton et al. (tion) found 175 HST/COS archival quasar spectra that at least partially covered the associated region for N V. Of those 175 quasars, 158 were radio-quiet, 16 were radio-loud, and 1 was unclear. Within those quasars, 59 intrinsic N V systems were found, but none of them were found within the spectrum of a radio-loud quasar. If systems are evenly distributed between radio-loud/radio-quiet quasars, there is less than a 1% probability of this occurring by chance, which would imply a dichotomy between radio-quiet and radio-loud quasars. However, half of the radio-loud quasars had FIRST radio images, which showed that over half of the morphologies of those radio-loud quasars were core-dominated, implying face-on orientations, high core fractions, and low inclination angles (as measured relative to the axis of the jet). This was consistent with a picture wherein sightlines with low inclination angles are

devoid of intrinsic N V absorbers. However, the question remains whether only radio-loud quasars with core-dominated morphologies are devoid of intrinsic N V absorbers, or if all radio-loud quasars show a dearth of intrinsic N V absorbers.

These findings led us to pursue observations of radio-loud quasars with a much greater range of morphologies, and hence inclination angles. Such a survey would allow us to determine if radio-loud quasars are fundamentally different from radio-quiet quasars, or if the sample of Culliton et al. (tion) was biased against finding N V absorbers in radio-loud quasars due to an unconscious bias in the HST archive to observe quasars with more face-on orientations, rather than edge-on. We select a sample 13 radio-loud quasars with a range of FIRST morphologies (see Figure 1) to investigate how radio properties and orientation can influence quasar winds. If radio-loud and radio-quiet quasars have similar wind structures, then we expect the detection of the wind through UV absorption lines in > 4 of the objects. The detection of an absorbing wind in < 2 of the objects will rule out to $> 90\%$ confidence that radio-quiet and radio-loud objects have similar wind structures and the available archival data somehow miss them. The complete absence of detections will rule out any similarity to 98% confidence and present severe challenges to the applicability of the disk-wind paradigm and orientation-based models to radio-loud objects.

This paper is organized as follows. §2 introduces our data selection and reduction. We present our results in §3. The paper is summarized in §4.

2 SAMPLE OF OBJECTS, OBSERVATIONS, AND DATA

The QSOs used for this study were selected from the SDSS Data Release 7 Quasar catalog from Schneider et al. (2010) based on the extensive work to compile quasar properties by Shen et al. (2011). We restrict the sample to radio-loud quasars ($\mathcal{R} \geq 10$, where \mathcal{R} is the radio-loudness parameter, defined as the ratio of the rest-frame radio and optical fluxes) with emission redshifts $z < 0.4$, and GALEX FUV magnitudes $m(FUV) < 18.3$. This ensures the sample is bright enough to observe with HST, while covering the N V $\lambda\lambda 1239, 1243$ doublet in the accessible spectral range.

The quasars were observed using the G130M or G160M gratings on the HST Cosmic Origins Spectrograph (COS). These gratings have resolving powers $R \sim 20,000$ (Green et al. 2012) corresponding to a velocity resolution of $\sim 15 \text{ km s}^{-1}$. Exposure times for our observations were chosen such that we obtain $S/N \geq 7$ per resolution element.

In Table 2, we present the observational details including the central wavelength of the grating, quasar emission redshift, V magnitude, and quasar rest-frame wavelength coverage. Redshifts are taken from Hewett & Wild (2010), with the exception of SDSS J110436.33+212417.8 and SDSS J154007.84+141137.0, which were taken from Abazajian et al. (2009). Four quasars were observed twice with the same gratings (SBS 0924+606B, 2E-3273, VV98-J150455.5+564920, and Q02349-014). The data were combined so as to enhance the S/N for these observations.

We list quasar properties such as black hole mass, M_{BH} , Eddington ratio, L/L_{Edd} , core-to-lobe ratio, R_{CL} ,

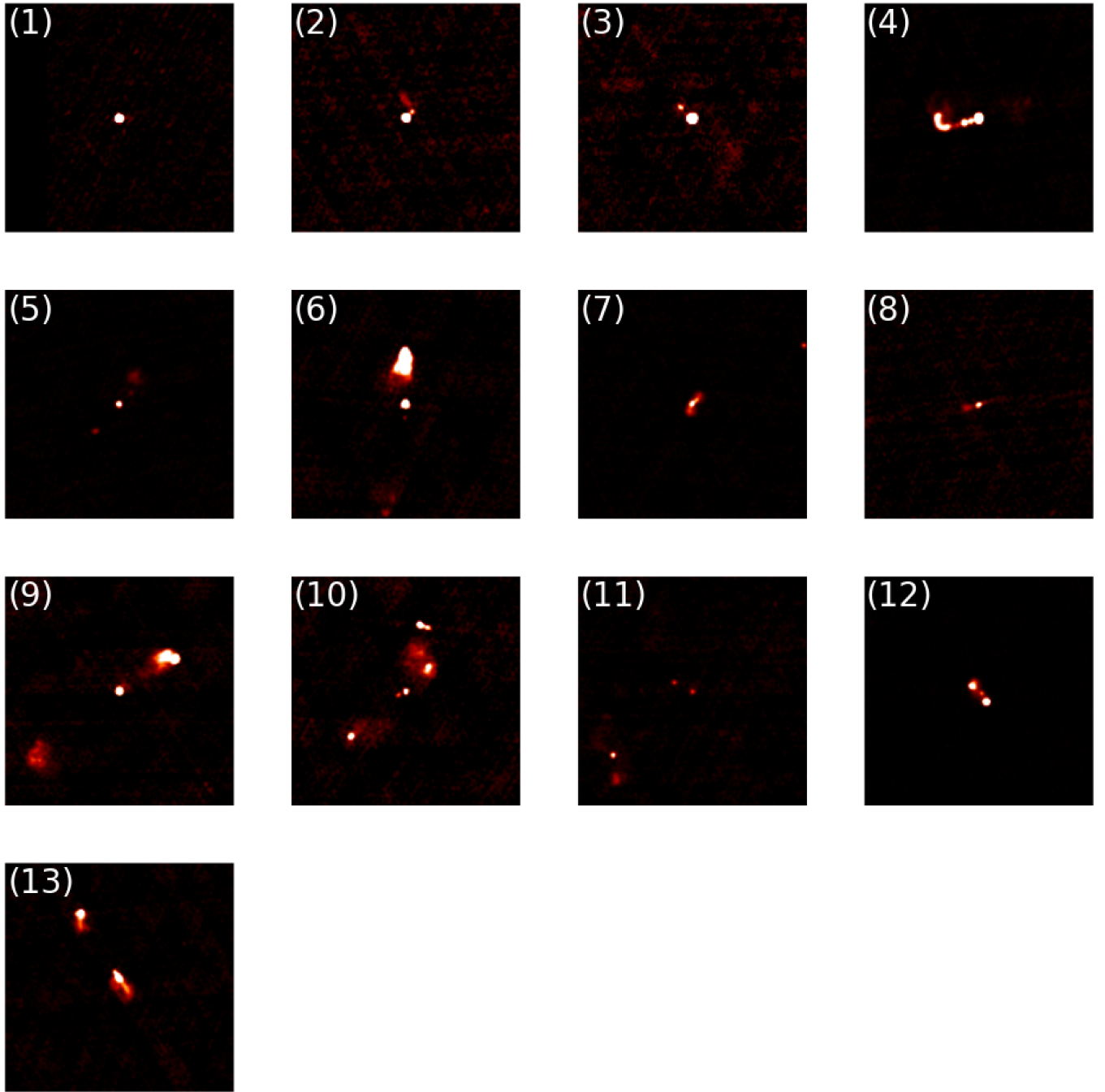


Figure 1. FIRST 1.4 GHz morphologies for the 13 radio-loud quasars in our sample. The images are ordered by increasing inclination, and the numbers in the upper left corner of each radio map corresponds to the index in Table 1.

inclination angle, i , and radio-loudness parameter, \mathcal{R} , in Table 1. The radio-loudness parameter is calculated as $L_\nu(6 \text{ cm})/L_\nu(2500 \text{ \AA})$. We use the convention set forth by Kellermann et al. (1989) and choose $\mathcal{R} \geq 10$ as our cut-off for radio-loud quasars. The core-to-lobe ratio is defined as the ratio of the core flux density to the lobe flux density, measured at an observed frequency of 5 GHz (Ganguly et al. 2001). This ratio provides a means of determining inclination that is not possible in radio-quiet quasars. We use the following semi-empirical relationship to calculate inclination,

adopted from Marin & Antonucci (2016):

$$i = 41.799 - 20.002(R_{CL}) - 4.603(R_{CL})^2 + 0.706(R_{CL})^3 + 0.663(R_{CL})^4 + 0.001(R_{CL})^5 \quad (1)$$

Marin & Antonucci (2016) showed this relationship holds for luminous quasars at an accuracy of $\sim 10\%$.

Figure 2 shows a possible scenario for the structure of a quasar system with various components labeled, adopted from Ganguly et al. (2001). In particular, we depict the outflow as green streamlines, and purple clumps. In principle,

Table 1. Quasar Properties

Index	Name SDSS J	z_{em}^a	M_{BH}^a ($10^8 M_\odot$)	L/L_{Edd}^a	R_{CL}^b (5 GHz)	i^c (°)	\mathcal{R} (6 cm/2500 Å)	# N v Systems
(1)	141628.66+124213.5	0.3349	15.2	0.04	14	15	132	0
(2)	114047.89+462204.8	0.1144	1.2	0.16	8.5	20	57	1
(3)	074906.50+451033.8	0.1923	3.5	0.08	2.2	35	82	0
(4)	122011.88+020342.2	0.2404	7.3	0.13	2.0	35	141	0
(5)	154007.84+141137.0	0.1197	2.9	0.03	1.1	41	34	1
(6)	091401.75+050750.6	0.3018	22.8	0.02	0.42	49	78	0
(7)	110436.33+212417.8	0.1877	3.7	0.06	0.35	50	63	0
(8)	110717.77+080438.2	0.2010	2.5	0.11	0.34	50	24	2
(9)	142735.60+263214.5	0.3638	45.2	0.02	0.30	51	107	4
(10)	093200.07+553347.4	0.2666	3.7	0.09	0.12	56	10	4
(11)	121613.62+524246.2	0.2698	1.6	0.12	< 0.08	> 58	29	0
(12)	092837.98+602521.0	0.2959	8.4	0.07	0.04	61	480	0
(13)	150455.56+564920.3	0.3589	7.3	0.09	< 0.01	> 69	260	3

^a Redshifts are taken from [Hewett & Wild \(2010\)](#), with the exception of SDSS J110436.33+212417.8 and SDSS J154007.84+141137.0, which were taken from [Abazajian et al. \(2009\)](#).

^b This core fraction represents the ratio of the radio flux of the core to that of the lobe(s).

^c These values are calculated using the equation for inclination angle found in [Marin & Antonucci \(2016\)](#) and the core to lobe ratio in column 6.

Table 2. Journal of HST Observations

QSO SDSS J	G130M			G160M			z_{em}^b	RA (J2000.0)	Dec. (J2000.0)	Mag. V	λ_{low}^c (Å)	λ_{high}^c (Å)
	T _{exp} (s)	PID	λ_c^a (Å)	T _{exp} (s)	PID	λ_c^a (Å)						
074906.50+451033.8	-	-	-	2156	14729	1600	0.1923 ± 0.0004	07:49:06.5000	+45:10:34.00	17.10	1180	1490
091401.75+050750.6	-	-	-	7947	14729	1577	0.3018 ± 0.0004	09:14:01.7684	+05:07:50.50	17.54	1062	1347
092837.98+602521.0	1163	11598	1291	1547	11598	1600	0.2959 ± 0.0004	09:28:37.984	+60:25:21.02	17.20	876	1385
	1148	11598	1309	1505	11598	1623						
093200.07+553347.4	-	-	-	5353	14729	1623	0.2666 ± 0.0004	09:32:00.0782	+55:33:47.41	17.57	1130	1422
110436.33+212417.8	-	-	-	2068	14729	1600	0.1877 ± 0.0014	11:04:36.3390	+21:24:17.87	17.38	1185	1496
110717.77+080438.2	-	-	-	1840	14729	1600	0.2010 ± 0.0004	11:07:17.7732	+08:04:38.28	17.35	1172	1480
114047.89+462204.8	2248	14729	1300	-	-	-	0.1144 ± 0.0004	11:40:47.9000	+46:22:05.00	16.14	1024	1294
121613.62+524246.2	-	-	-	2240	14729	1623	0.2698 ± 0.0004	12:16:13.6535	+52:42:46.18	17.79	1127	1418
122011.88+020342.2	2052	13852	1291	2589	13852	1600	0.2404 ± 0.0004	12:20:11.885	+02:03:42.22	15.97	913	1433
141628.66+124213.5	-	-	-	7964	14729	1600	0.3349 ± 0.0004	14:16:28.6563	+12:42:13.58	17.54	1054	1331
142735.60+263214.5	1075	12603	1291	5077	14729	1600	0.3638 ± 0.0004	14:27:35.6003	+26:32:14.65	16.00	859	1303
	1170	12603	1327	-	-	-						
150455.56+564920.3	2047	12276	1327	8695	14729	1600	0.3589 ± 0.0004	15:04:55.5624	+56:49:20.30	17.20	833	1308
	3116	12276	1291	-	-	-						
154007.84+141137.0	2064	14729	1300	-	-	-	0.1197 ± 0.0016	15:40:07.8470	+14:11:37.12	17.15	1020	1289

^aCOS gratings have various tilts so we present the central wavelength of the spectrum. The central wavelengths have the following wavelength coverage: 1291, 1134 Å–1431 Å; 1300, 1144 Å–1441 Å; 1309, 1154 Å–1450 Å; 1327, 1172 Å–1469 Å; 1577, 1386 Å–1751 Å; 1600, 1409 Å–1774 Å; and 1623, 1432 Å–1798 Å.

^bRedshifts are taken from [Hewett & Wild \(2010\)](#), with the exception of SDSS J110436.33+212417.8 and SDSS J154007.84+141137.0, which were taken from [Abazajian et al. \(2009\)](#).

^cWavelength coverage is reported in the quasar rest-frame.

sightlines that pass through these structures would show the outflow in absorption. Superimposed on the schematic, we show the sightlines¹ for the objects in our sample. Red indicates a sightline for those quasars in which we see outflows.

Blue indicates a sightline for those quasars where an outflow is not detected. A dashed sightline indicates one in which the radio core is not detected. Such a sightline could be more inclined than shown. The numbers correspond to the quasars indexed in Table 1.

¹ In practice, there is no one sightline coming from the quasar. Instead, there are parallel rays originating from all parts of the BELR and continuum region. These rays make up a “cylinder of sight,” rather than one sightline. However, for our purposes here, a sightline refers to the direction of the observer from the origin

at the center of the quasar, and is encapsulated by the cylinder of sight.

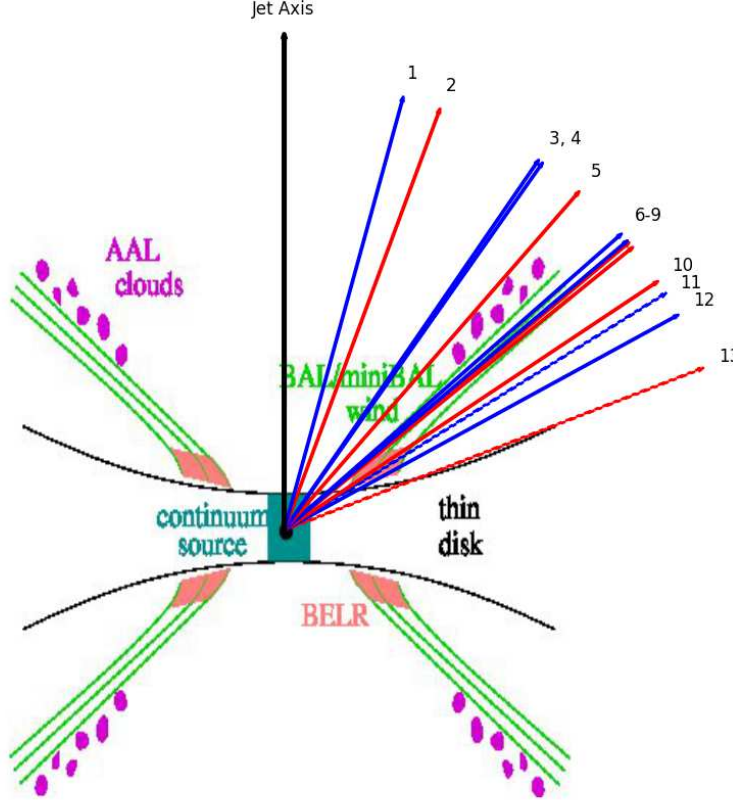


Figure 2. A possible scenario for the structure of a quasar system with various components labeled. In particular, we depict the outflow as green streamlines, and purple clumps. In principle, sightlines that pass through these structures would show the outflow in absorption. Superposed on the schematic, we show the sightlines for the objects in our sample. Inclination angle is measured with respect to the polar axis. Red indicates objects for which we see outflows. Blue indicates objects where an outflow is not detected. A dashed sightline indicates one in which the radio core is not detected. Such a sightline could be more inclined than shown. The numbers correspond to the quasars indexed in Table 1.

3 RESULTS AND DISCUSSION

We searched for N V absorption across the entire available spectra of the 13 quasars up to $10,000 \text{ km s}^{-1}$ redward of the N V emission redshift. The HST/COS spectra of the 13 objects in our sample can be seen in Figures 3 and 4. In each panel, we show only the portion of the spectrum covering the Ly α and N V emission lines. When detected, Ly α absorption is highlighted in red and N V absorption is highlighted in blue. The sequence of ordinal numbers progresses by increasing inclination angle, corresponding to Table 1. In total, we found 15 intrinsic N V systems within the spectra of 6 of the 13 quasars. All such systems were found within 2000 km s^{-1} of the quasar emission redshift, well within the associated region of the quasar. The systems are detailed in

Table 3, including the quasar spectrum within which the system was discovered in, the emission redshift of the quasar, z_{em} , the absorption redshift of the system, z_{abs} , and the velocity offset of the system, v_{offset} . Two quasars had one system each within their spectra, one quasar had two systems within its spectrum, one quasar had three systems within its spectrum, and two quasars each had four systems within their spectra.

In order to determine if the tendency of the N V systems to cluster in a given quasar's spectra implied preferred sightlines to the quasars within which intrinsic systems form, we performed bootstrapping statistical trials. Such a preferred sightline would indicate a given geometry increasing the likelihood of finding an intrinsic system, rather than if the dis-

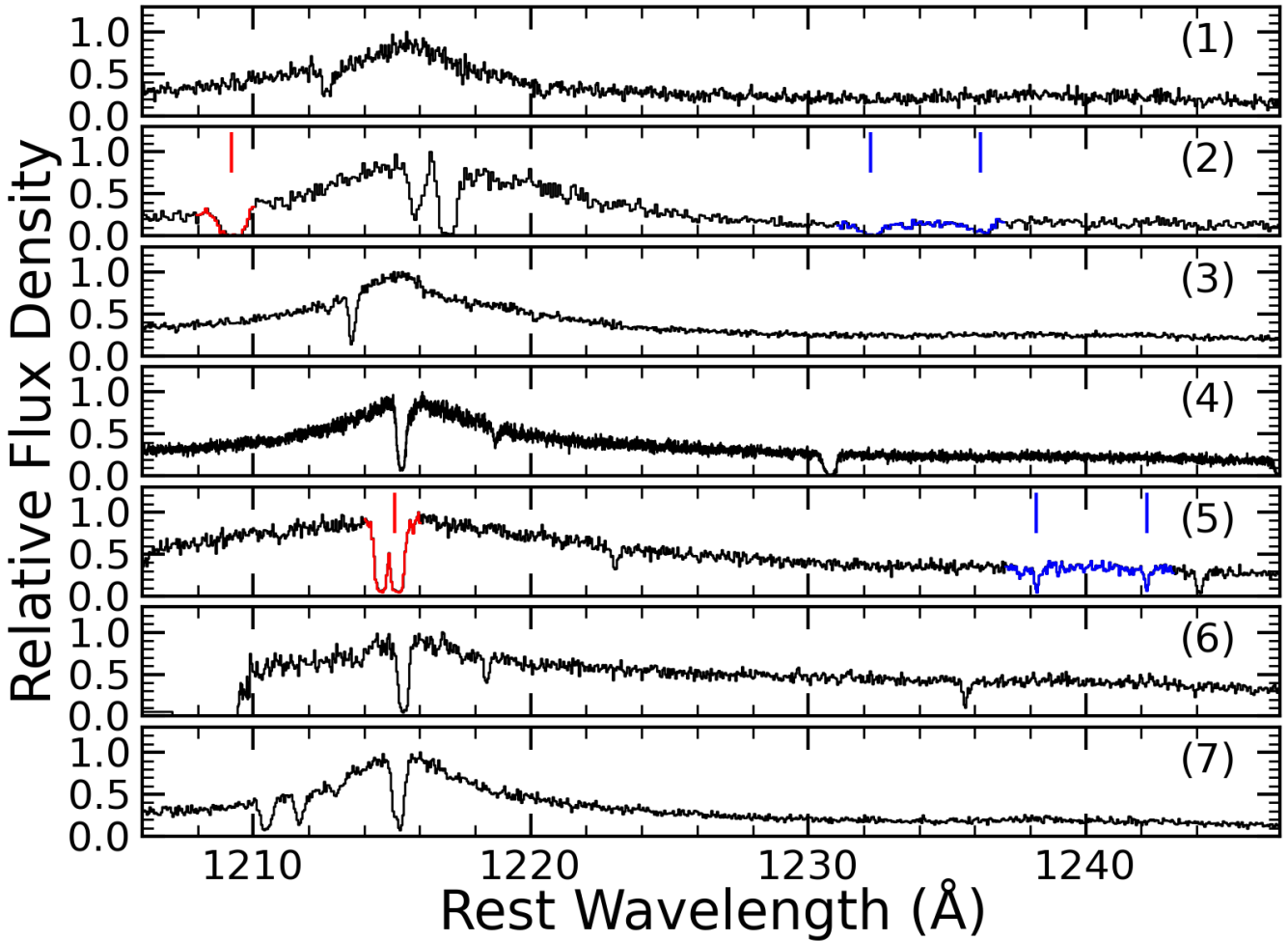


Figure 3. HST/COS spectra of 7 of the 13 objects in our sample. The spectra of objects 8–13 are in Figure 4. In each panel, we show only the portion of the spectrum covering the Ly α and N v emission lines. When detected, Ly α absorption is highlighted in red and N v absorption is highlighted in blue. The sequence of ordinal numbers progresses by increasing inclination angle, corresponding to Table 1.

Table 3. System properties

Index	Name SDSS J	i (°)	z_{em}	z_{abs}	$v_{\text{offset}}^{\text{a}}$ km s^{-1}
(2)	114047.89+462204.8	20	0.1144	0.1083	-1614
(5)	154007.84+141137.0	41	0.1197	0.1197	-141
(8)	110717.77+080438.2	50	0.2010	0.1990 0.2010	-506 0
				0.3577	-1347
(9)	142735.60+263214.5	51	0.3638	0.3589 0.3597 0.3633	-1082 -915 -105
				0.2625	-947
(10)	093200.07+553347.4	56	0.2666	0.2642 0.2649 0.2659	-565 -380 -152
				0.3540	-1075
(13)	150455.56+564920.3	> 69	0.3589	0.3568 0.3578	-464 -254

^a Negative velocity offsets indicate that the absorber is to the blue of the emission redshift.

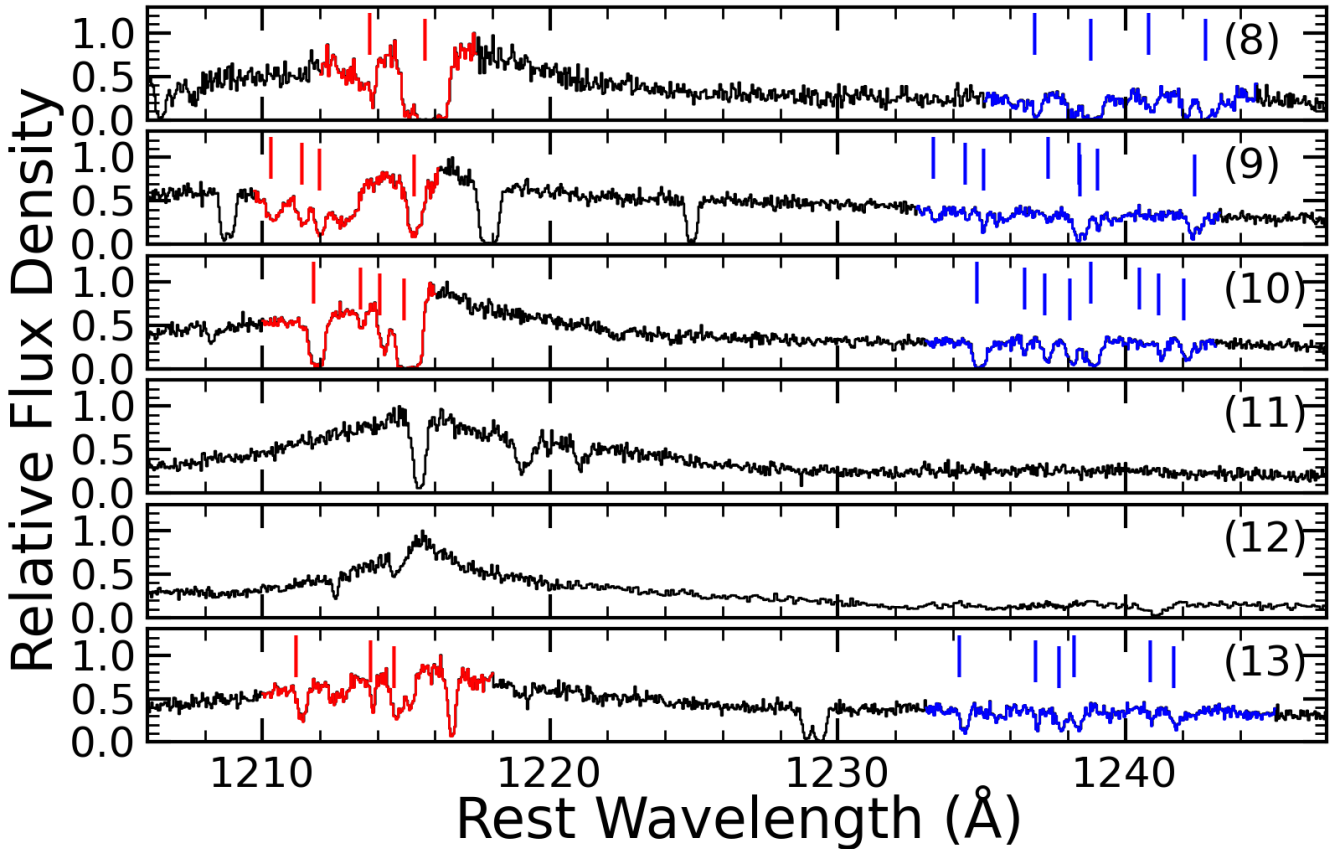


Figure 4. HST/COS spectra of 6 of the 13 objects in our sample. The spectra of objects 1–7 are in Figure 3. In each panel, we show only the portion of the spectrum covering the Ly α and Nv emission lines. When detected, Ly α absorption is highlighted in red and Nv absorption is highlighted in blue. The sequence of ordinal numbers progresses by increasing inclination angle, corresponding to Table 1.

tribution of intrinsic systems was consistent with random chance. In these trials, 15 systems were randomly placed within 13 quasars to determine the random distribution (i.e., how many quasars contained one system, how many with 2 systems, etc.). This trial was repeated 100,000 times, and the results were totaled.

When compared with our sample, the results of these trials showed that a large number of quasars with zero systems was rare. The average distribution of quasars had 3.9 quasars with no intrinsic systems, fewer than the 7 that were observed in our sample. The trials resulted in at least 7 quasars with no systems only 1.1% of the time. The trials had the opposite problem with quasars with one or two systems. 98% of the time, the trials resulted in two or more quasars with only one system, while they resulted in at least one quasar with two systems 97% of the time. The average distribution had one quasar with three systems, just as we found, and three or more systems were found in at least one quasar 72% of the time. Finally, the average distribution had fewer quasars with four systems within a given quasar, 0.26, than the two quasars we observed with four systems

each. The trials resulted in at least three quasars with four systems each only 1.3% of the time. With intrinsic Nv systems clustering in the spectra of a few quasars despite the low probability of such an event occurring randomly, this distribution of systems heavily implies that finding systems depends on preferred sightlines to the quasar, rather than these systems clustering by chance.

3.1 Dependence on Inclination Angle

If we compare the number of systems within the spectra of the quasars to the sightline to the given quasars, we find that decreasing core-to-lobe ratio and increasing inclination angle results in an increasing number of systems per quasar. Culliton et al. (2014) found no Nv systems within any radio-loud quasars, where the majority of the quasars had core-dominated morphologies, implying low inclination angles. The two quasars with only one system each, SDSS J114047.89+462204.8 and SDSS J154007.84+141137.0, had core-to-lobe ratios of 8.5 and 1.1, and inclination angles of 20° and 41°, respectively. The quasar with two systems,

[h]

Table 4. Bootstrapping Trial Results

Number of Quasars with N Systems	$N = 0$	$N = 1$	$N = 2$	$N = 3$	$N = 4$
Survey Results, $S(N)$	7	2	1	1	2
Trial Averages, $\bar{T}(N)$	3.9	4.9	2.9	1.0	0.26
Fraction of Trials with $T(N) \geq S(N)$	1.1%	98%	97%	72%	1.3%

SDSS J110717.77+080438.2, was found to have a core-to-lobe ratio of 0.34 and an inclination angle of 50° . The quasar with three systems, SDSS J150455.56+564920.3, had a core-to-lobe ratio of < 0.01 and an inclination angle of $> 69^\circ$. The two quasars with four systems each, SDSS J093200.07+553347.4 and SDSS J142735.60+263214.5, had core-to-lobe ratios of 0.12, 0.30, and inclination angles of 56° and 51° , respectively. The preferred sightlines to radio-loud quasars for intrinsic N v absorbers are thus those with high inclination angles.

However, despite the importance of the inclination angle, it should be noted that inclination angle is not the only factor in determining whether a quasar's spectrum will contain intrinsic N v absorbers. If a laminar outflow existed above a fixed, universal inclination angle that is based on the properties of the quasar, we would have a fixed boundary between the region in which high inclination angle sightlines result in the presence of intrinsic N v absorbers, and the low inclination angle sightlines that are devoid of such absorbers. Such a laminar outflow is ruled out by our observations. In this project, we observed quasars with a wide range of orientations, from nearly face-on, core-dominated quasars, to quasars with distinct radio lobes that are nearly edge on, as can be seen in Figure 2 and Table 1. Two of the quasars with the highest inclination angles, SDSS J121613.62+524246.2 and SDSS J092837.98+602521.0 did not contain any N v absorption. Similarly, there are quasars whose redshift, black hole mass, Eddington luminosity, core-to-lobe ratio, inclination angle, and radio-loudness parameter are nearly identical, such as SDSS J110717.77+080438.2 and SDSS J110436.33+212417.8, yet one has N v absorption, while the other does not. If a laminar outflow existed, we would expect that two such similar quasars would have the same opening angles to their outflows, and thus they would either both show intrinsic absorption, or they both would not. Additionally, SDSS J114047.89+462204.8 is a quasar with *low* inclination that *does* have an intrinsic N v system, meaning that although low inclination quasars with systems are rare, the polar regions of quasars are not completely devoid of intrinsic N v absorbing material. It seems unlikely that this one particular quasar has a range of inclination angles for a laminar outflow that must extend to $i \leq 20^\circ$, when other quasars do not have N v absorbing material at $i < 40^\circ$, despite this quasar having properties that are not significantly different than any of the others. Such discrepancies imply that there is instead a clumpy outflow with sporadic ejections of material at various inclination angles, rather than a laminar outflow in which a quasar ejects material within a range of inclination angles. These findings also imply that while inclination angle does affect the probability of finding one or more intrinsic N v systems within their spectra, it does not guarantee the presence of intrinsic

N v absorbers. Instead, *the probability* of finding one or more intrinsic N v absorption systems is a function of inclination angle, with that probability increasing with increasing inclination angle. These results are indicative of an equatorial wind disk model with the outflows being sporadic bursts of material embedded in a hotter, sparser medium, provided the opening angle of the wind is not too large.

3.2 Dependence on Radio-Loudness

As seen above, and in Culliton et al. (2018) and Culliton et al. (tio), as the radio-loudness parameter of a quasar increases, the maximum velocity and equivalent width of the systems found in that quasar was found to decrease. Winds are therefore weaker, less dense, and slower than those of quasars with smaller values of the radio-loudness parameter, \mathcal{R} . Radio-quiet quasars are able to accelerate N v systems to nearly 5000 km s^{-1} , but the highest speeds found in either this sample or Culliton et al. (tio) for N v systems was 1614 km s^{-1} . Only 4 of 15 systems exceeded 1000 km s^{-1} . Therefore, the higher the radio-loudness parameter, the less efficient the quasar is at accelerating winds, and the less material gets accelerated as a wind. A potential explanation for this comes from a modified version of the spin paradigm (Chiaberge & Marconi 2011) in which the radio-loudness of an AGN is determined not only by the spin, but also by the mass of the supermassive black hole. The faster a black hole spins, the smaller the radius of the inner-most stable orbit (ISCO). The temperature of the disk is inversely proportional to radius, so as a black hole spins faster, the material at the ISCO becomes hotter, and the SED of the quasar becomes harder. This could lead to the X-ray radiation ionizing the wind to such an extent that few transitions remain within the ion, preventing efficient line driving of the gas, and potentially preventing the wind from being accelerated to as high of a degree as in radio-quiet quasars.

This could lead to two competing effects. As radio-loudness increases, the probability of finding an intrinsic N v system in the spectra of quasars decreases, but as inclination angle increases, the probability of finding an intrinsic N v system in the spectra of quasars increases. Of the 13 quasars in our sample, only five have $\mathcal{R} > 100$. Of those five quasars, only two have N v systems. The radio-loudness parameter of the two quasars are $\mathcal{R} = 107$ and $\mathcal{R} = 260$, while the inclination angles are $i = 51^\circ$ and $i > 69^\circ$, respectively. In these two cases, it would appear that the high inclination angle of the quasar increasing the probability of finding an intrinsic system was the overriding factor in whether the quasar would have an intrinsic system within its spectra. If you remove these two quasars with intrinsic N v systems from the sample, then the quasars with intrinsic N v systems

in their spectra all have relatively low radio-loudness parameters ($\mathcal{R} < 60$), while those quasars with high radio-loudness parameters ($\mathcal{R} > 60$) do not have intrinsic Nv systems. With those two quasars removed, Kolmogorov-Smirnov and Anderson-Darling tests both show that there is a $< 2\%$ chance that the radio-loudness of the quasars with systems come from the same distribution as the radio-loudness parameter of quasars without systems.

Of the three quasars with both $\mathcal{R} > 100$ and no intrinsic Nv systems in their spectra, two have low inclination angles ($i = 15^\circ$ and $i = 35^\circ$). As such, it is unlikely they would have intrinsic systems within their spectra even if they had lower radio-loudness parameters. The final quasar with a large radio-loudness parameter ($\mathcal{R} = 480$) has an inclination angle of $i = 61$. At such an inclination, it would be assumed that this quasar would be likely to have an intrinsic system. However, the high radio-loudness parameter could prevent winds from forming around this high inclination quasar. The results of these competing effects is further illustrated by the fact that of the five quasars with the lowest radio-loudness parameter, four have intrinsic systems, despite the fact that two of the four quasars have relatively low inclination angles. Additionally, consider Quasars 4 and 5 (SDSS J122011.88+020342.2 and SDSS J154007.84+141137.0) from Table 1. They have similar inclination angles, but the black hole mass of Quasar 4 is over twice that of Quasar 5. The Eddington ratio for Quasar 4 is over three times that of Quasar 5. It would be expected that more material would be ejected by Quasar 4, as well as accreted, which would seemingly make the likelihood of finding a system in Quasar 4 higher than in Quasar 5, but Quasar 5 has a system while Quasar 4 does not. This could be an effect of Quasar 4 having a radio-loudness parameter over four times that of Quasar 5. The most likely quasars to have an intrinsic Nv system within its spectra are therefore quasars that have *both* a high inclination angle *and* a relatively low radio-loudness parameter. More observations of radio-loud quasars with known radio morphologies could confirm this trend.

4 SUMMARY

Using spectra of 13 low-redshift, radio-loud quasars, we construct a sample with a wide range of inclination angles and core-to-lobe ratios. We identified 15 intrinsic Nv absorption systems within 6 of the 13 quasars. We determined that finding intrinsic Nv systems within the spectra of quasars is heavily dependent on the inclination angle of the quasar, rather than systems appearing by ran-

dom chance. The preferred sightlines to radio-loud quasars are those with high inclination angles and relatively low radio-loudness. However, inclination angle alone does not determine the presence or absence of intrinsic systems. Two quasars can have otherwise identical properties, yet exhibit Nv absorption in one, but not the other. This is highly indicative of an outflow that is patchy or clumpy, rather than a laminar outflow that exists above a given inclination angle, and that the likelihood of finding one or more intrinsic Nv systems is anti-correlated with the radio-loudness parameter.

ACKNOWLEDGEMENTS

This work was supported by NSF grant AST-0807993
TM acknowledges support from JSPS KAKENHI Grant Number 15K05020

References

- Abazajian K. N., et al., 2009, *ApJS*, **182**, 543
- Anderson S. F., Weymann R. J., Foltz C. B., Chaffee Jr. F. H., 1987, *AJ*, **94**, 278
- Barlow T. A., Hamann F., Sargent W. L. W., 1997, in Arav N., Shlosman I., Weymann R. J., eds, Astronomical Society of the Pacific Conference Series Vol. 128, Mass Ejection from Active Galactic Nuclei. p. 13 ([arXiv:astro-ph/9705048](https://arxiv.org/abs/astro-ph/9705048))
- Chiaberge M., Marconi A., 2011, *MNRAS*, **416**, 917
- Culliton C., Charlton J., Eracleous M., Ganguly R., Misawa T., 2018, *MNRAS*
- Culliton C., Roberts A., DeMarcy B., Muzahid S., Charlton J. C., Ganguly R., 2018, In Preparation, *MNRAS*
- Di Matteo T., Springel V., Hernquist L., 2005, *Nature*, **433**, 604
- Foltz C. B., Weymann R. J., Peterson B. M., Sun L., Malkan M. A., Chaffee Jr. F. H., 1986, *ApJ*, **307**, 504
- Ganguly R., Bond N. A., Charlton J. C., Eracleous M., Brandt W. N., Churchill C. W., 2001, *ApJ*, **549**, 133
- Green J. C., et al., 2012, *ApJ*, **744**, 60
- Hewett P. C., Wild V., 2010, *MNRAS*, **405**, 2302
- Hopkins P. F., Torrey P., Faucher-Giguère C.-A., Quataert E., Murray N., 2016, *MNRAS*, **458**, 816
- Kellermann K. I., Sramek R., Schmidt M., Shaffer D. B., Green R., 1989, *AJ*, **98**, 1195
- Marin F., Antonucci R., 2016, *ApJ*, **830**, 82
- Sargent W. L. W., Boksenberg A., Steidel C. C., 1988, *ApJS*, **68**, 539
- Schneider D. P., et al., 2010, *AJ*, **139**, 2360
- Shen Y., et al., 2011, *ApJS*, **194**, 45
- Suresh J., Bird S., Vogelsberger M., Genel S., Torrey P., Sijacki D., Springel V., Hernquist L., 2015, *MNRAS*, **448**, 895
- Weymann R. J., Williams R. E., Peterson B. M., Turnshek D. A., 1979, *ApJ*, **234**, 33
- Young P., Sargent W. L. W., Boksenberg A., 1982, *ApJS*, **48**, 455